Biomaterials Advances 185 (2026) 214851

Contents lists available at ScienceDirect

Biomaterials Advances

journal homepage: www.journals.elsevier.com/materials-science-and-engineering-c

Engineering of bacterial cellulose-based vascular grafts for small-diameter applications

Deborah Fusco [a,b], Noor Christiaens [a,b], Elia Pederzani [c], Sara Martinazzi [d], Giuseppe Isu [a,b], Florian Meissner [a,b], Jules Miazza [a], Urs Zenklusen [a], Michael Gregor [d], Luca Koechlin [a], Alessia Pisanu [a,b], Marcello Raimondi Lucchetti [e], Gianfranco B. Fiore [d], Monica Soncini [d], Katharina Glatz [f], Alessio Rungatscher [e], Bernhard Winkler [g], Friedrich Eckstein [a,b], Anna Marsano [a,b,*]

[a] Department of Surgery, University Hospital Basel, Basel, 4031, Switzerland
[b] Department of Biomedicine, University Hospital Basel and University of Basel, Basel, 4031, Switzerland
[c] Department of Anaesthesiology, University Hospital of Basel, Basel, 4031, Switzerland
[d] Department of Electronics, Informatics and Bioengineering, Politecnico di Milano, Milano, 20133, Italy
[e] Department of Surgery, University of Verona, Verona, 37126, Italy
[f] Institute of Pathology, University Hospital Basel, University of Basel, Basel, 4031, Switzerland
[g] Department of Biomedical Research, Medical University of Vienna, Vienna, 1091, Austria

ARTICLE INFO

Keywords:
Tissue engineering
biomaterials
small-diameter vascular graft
bacterial cellulose
biocompatibility
mechanical characterization
ISO

ABSTRACT

Cardiovascular diseases remain the leading cause of mortality worldwide, necessitating advanced revascularization strategies such as coronary artery bypass grafting (CABG). While autologous vessels like the saphenous vein are commonly used, their limited availability, their potential maladaptation to the arterial environment, and the suboptimal performance of synthetic alternatives underscores the urgent demand for innovative small-diameter grafts. Grafts made of Bacterial Cellulose (BC), synthesized by *Acetobacter xylinum*, have gained attention due to its excellent biocompatibility, mechanical integrity, and *in vivo* patency. However, clinical translation is hindered by inconsistent fabrication processes that result in graft mismatched dimensions and variable mechanical performance. This study presents an optimized and reproducible culture method for producing BC-based grafts with clinically relevant dimensions (4 mm inner diameter and 15 cm length). The grafts were evaluated morphologically, biologically and mechanically according to ISO-10993 and ISO-7198 standards, using human saphenous veins as a benchmark. While the veins exhibited high variability in structure (inner diameter: 2.6 ± 0.7 mm; outer diameter: 4.9 ± 1.3 mm) and performance (*e.g.*, burst pressure: 577.4 ± 631.3 mmHg), the BC grafts demonstrated consistent morphology (inner diameter: 4.00 mm; outer diameter: 4.92 ± 0.10 mm) and favorable and more reproducible mechanical properties (*e.g.* burst pressure: 306.6 ± 96.04 mmHg).

In vitro assays confirmed effective bacterial residue removal, low thrombogenicity and preserved the biocompatibility of the cellulose network. Subcutaneous implantation of BC grafts induced a mild inflammatory response, and showed no signs of calcification, in contrast to Gore-tex implants.

These findings emphasize the potential of BC grafts as reliable, scalable, and clinically relevant alternatives for vascular substitutes, including pediatric applications, and underscore the importance of standardized production for translational success.

1. Introduction

Cardiovascular diseases (CVD) remain the leading cause of mortality worldwide [1,2], with vascular occlusion often requiring interventions such as [3] percutaneous coronary interventions and coronary bypass grafting (CABG). CABG alone accounted for more than half of adult

* Corresponding author at: Department of Biomedicine, University Hospital Basel, University of Basel, Basel, 4031, Switzerland.
E-mail address: anna.marsano@usb.ch (A. Marsano).

https://doi.org/10.1016/j.bioadv.2026.214851
Received 31 October 2025; Received in revised form 17 March 2026; Accepted 27 March 2026
Available online 31 March 2026

cardiac surgeries in the United States in 2019 [1]. In parallel, the rising prevalence of peripheral arterial disease, driven by aging populations and chronic comorbidities, underscores the continued demand for effective vascular grafts, including for the treatment of chronic limb-threatening ischemia [4,5]. Autologous grafts, including the saphenous vein (SV) and internal mammary artery, are the preferred conduits for CABGs, and other vascular procedures such as arteriovenous shunts, due to their biocompatibility and clinical performance [3]. The SV, in particular, is widely used for its ease of harvest, and sufficient length [6,7]. However, up to one-third of patients lack suitable autologous vessels due to prior surgeries or vascular diseases [8]. Furthermore, veins used as arterial substitutes are prone to long-term complications, including mechanical mismatch, aneurysmal dilation, intimal hyperplasia, and early occlusion, often requiring reintervention within 10 years [3,7].

Synthetic vascular grafts such as expanded polytetrafluoroethylene (ePTFE, Gore-tex®) and polyethylene terephthalate (Dacron®) perform well in large-diameter applications (>6 mm internal diameter), but exhibit poor patency in small-diameter grafts (<5 mm internal diameter) [3,9]. These limitations have driven the development of biologically derived and tissue-engineered vascular grafts that better replicate native morphological, mechanical and biological properties and offer long-term performance, including potential use in pediatric patients. Decellularization of xenogeneic vessels reduces immunogenicity while maintaining biological cues [10–12]. A notable example is Humacyte®, which uses human vascular cells seeded onto a biodegradable scaffold followed by decellularization. It is currently in Phase II and III clinical trials for limb large-diameter bypass applications and has demonstrated promising preclinical outcomes as CABG substitute [13–15].

Bacterial Cellulose (BC), an extracellular polysaccharide produced by *Acetobacter xylinum* and related strains [16,17], has emerged as a promising material for vascular tissue engineering due to its high mechanical strength, nanofibrillar structure, water retention capacity, and excellent biocompatibility [18–20]. Originally used in food and paper industries, BC has since gained clinical interest in applications including artificial skin, wound dressing, dental membranes, and aortic valves [20,21]. In preclinical vascular studies, BC-based grafts have shown encouraging patency and *in vivo* integration [22,23]. BC results in limited activation of the coagulation cascade and favorable hemocompatibility as well as in *in vivo* revascularization, supporting endothelial cell adhesion and tissue remodeling [22,24,25]. Despite these promising biological attributes, several critical challenges continue to hinder the clinical translation of BC vascular grafts.

A major limitation is the lack of controlled and standardized fabrication methods. BC synthesis is highly sensitive to fermentation parameters, including bacterial inoculum density, oxygen availability, temperature, pH, carbon source composition, that directly influence cellulose deposition [26,27]. However, many studies report limited process control and a lack of standardized mechanical and biological characterization, which complicates cross-study comparisons and regulatory acceptance. Functionally, BC grafts often exhibit mismatches in wall thickness relative to native coronary arteries, which may impair hemodynamic performance and long-term outcomes [22–24]. In addition, most fabrication strategies yield grafts of limited length, typically below 10 cm, with only a few reports achieving lengths up to 14 cm, constrained by the dimensions of the silicone tube holder [22,28].

Previous BC graft fabrication methods, including closed static or rotating bioreactor chambers relying on oxygen gradients [10] or open air-liquid interfaces [23], suffer from inconsistent oxygen supply and contamination risks, and limited scalability [29,30]. Static single- or double-tube system-based bioreactors were developed to enhance oxygen delivery and produce non-layered walls, which are known to be prone to delamination, with improved mechanical properties [28,30]. Alternative approaches rely on BC formation at the inner lumen of oxygen-permeable silicone molds or polydimethylsiloxane tubes, yielding conduits with oriented fibers but limited scalability [25].

Rolling or folding of pre-formed BC sheets and post-processing of bulk cellulose blocks have also been explored as cost-effective processes, yet these methods lack robustness, reproducibility, and clinically relevant size [29,30]. Critically, many studies do not implement systematic control of fermentation, quality criteria, resulting in variable cellulose deposition and mechanical properties.

In this study, we introduce a new closed single-chamber culture system that delivers high-concentration oxygen through an oxygen-permeable silicone tube, enabling sterile, reproducible, and controlled production of long (15 cm after harvest), small inner diameter (4 mm) BC vascular grafts.

Our approach integrates standardized bacteria cell banks, defined quality control criteria to support consistent cellulose deposition, and controlled fermentation protocols. Graft morphology, biocompatibility, and mechanical performance were evaluated according to ISO-10993 and ISO-7198 standards. Mechanical properties of BC grafts were benchmarked against human SV grafts.

2. Material & methods

2.1. Bacteria and culture media

Acetobacter Xylinum ATCC© 70018™ was employed to produce BC-based vascular grafts. A starter medium of Hassid-Barker was made per 1 l of milliQ water containing 10% sucrose (Sigma Aldrich, USA), 0.25% yeast extract (Sigma Aldrich, USA), 0.5% K_2HPO_4 (Sigma Aldrich, USA), 0.6% $(NH_4)_2SO_4$ (Sigma Aldrich, USA), and 0.2% $MgSO_4$ (Sigma Aldrich, USA). Fermentation medium for the BC-based vascular graft production consists of 4% D-fructose (Sigma Aldrich, USA), 0.5% yeast extract (Sigma Aldrich, USA), 0.33% Na_2HPO_4 (Sigma Aldrich, USA), 0.1% K_2HPO_4 (Sigma Aldrich, USA), 0.025% $MgSO_4$ (Sigma Aldrich, USA), 0.5% proteose peptone (Sigma Aldrich, USA). The media pH was adjusted to 5.5 using ≥99.9% acetic acid (Sigma Aldrich, USA).

2.2. Bacteria propagation and fermentation process

BC-based vascular graft production was carried out with two-step cultivation process consisting of microbial propagation followed by fermentation in a custom-made bioreactor (Supplementary Fig. 1A–C). Prior to production, a Master Cell Bank (MCB) and a Working Cell Bank (WCB) were established to ensure the reproducibility and consistency of the bacterial cultures throughout the manufacturing process. This strategy was essential to minimize the risk of contaminations and genetic variation, such as the loss of cellulose-producing capability, which may arise from prolonged continuous culturing [32]. Bacterial cultures were maintained for a maximum of two months, after which a new vial from the WCB was thawed, expanded, and used for production.

During the propagation step, *Acetobacter xylinum* was incubated under shaking conditions at 150 rpm from 48 to 72 h at 28 °C in Hassid-Barker medium [33] adjusted to pH: 5.5 and supplemented with 0.8% cellulase from Trichoderma reesei (Sigma Aldrich, USA).

Prior to fermentation phase, each newly expanded WCB batch of *Acetobacter xylinum* was subjected to quality control assessment, including evaluation of static bacterial cellulose production, bacterial cell count, and colony formation capacity and morphology (Supplementary Fig. 1A). These tests ensured adequate cellulose-producing capacity and culture integrity.

At the end of the propagation, Acetobacter Xylinum was transferred into a rotating custom-made culture chamber with a fermentation medium, composed by Hassid-Barker medium with the supplementation of 0.5% v/v proteose peptone (Sigma Aldrich, USA), and D-fructose instead of sucrose (Sigma Aldrich, USA) as carbon source. Before fermentation, *Acetobacter Xylinum* was first cultivated on a static plate to assess its ability to produce cellulose, ensuring its suitability for the fermentation process. Additionally, bacterial samples were plated on agar plates for morphological evaluation of the colonies, allowing the detection of

potential contaminations (*e.g.*, fungi, bacteria) (Supplementary Fig. 1A). To minimize variability in cellulose deposition and to standardize the production process, a fixed amount of bacteria corresponding to an Optical Density ≈ 0.1 (BioTek Synergy H1, Agilent, USA) was transferred in each rotating culture vessel (Supplementary Fig. 1A) and further culture up to 5 days (fermentation phase) at the speed of 1.7 rpm.

Up to four BC-based vascular grafts were generated in parallel by cellulose deposition around oxygen permeable platinum cured silicon tubes (wall thickness: 0.5 mm) (Maagtechnic, Switzerland) through which oxygen was supplied from a closed not-gas permeable tube loop with a reservoir of oxygen filled up with 100% of oxygen (Supplementary Fig. 1B–C), refreshed every 24 h. The oxygen drop (% O_2 after filling - % O_2 before filling) following 24 h was 34.07 ± 4.53% (Supplementary Fig. 1D). Fermentation process lasted 5 days in a bacteriological incubator (Thermo Scientific, USA) at 28–30 °C. The resultant BC-based grafts were subjected to alkaline treatment for 12 days to remove bacterial remnants from the cellulose fibrillar network [23]. Briefly, the newly fabricated vascular grafts were immersed in a 0.7 N NaOH solution for 8 days, with daily replacement of the solution. On day 8, the grafts were incubated at 60 °C for 4 h in fresh 0.7 N NaOH. Subsequently, the grafts were transferred to a 0.3 N NaOH solution and maintained for an additional 4 days, with daily solution changes. The vascular grafts were then thoroughly rinsed and immersed in Milli-Q water for 4 days, with daily water replacement. Finally, on day 5, the grafts were sterilized by autoclaving in Milli-Q water.

2.3. Collection and preparation of human Saphenous Vein (SV)

Human donor material from SV was anonymously obtained as surgical leftovers (Request number 2020-01197) from patients undergoing CABG at Basel University Hospital (Switzerland). The donors included 40 male patients and 1 female patient. After surgical procedures, the venous residues were collected immediately and stored at 4 °C in phosphate-buffered saline (PBS) (Sigma-Aldrich, USA). Subsequently, the grafts were rinsed with Hank's balanced salt solution (HBSS) (Sigma-Aldrich, USA), and if present, surplus fat or connective tissue was excised. Any surgical metal clips and/or sutures from clipped side branches were left *in situ* (as they are typically preserved during conventional CABG). All samples used for mechanical testing and histology were processed within 24 h after surgery [34].

2.4. Tensile strength measurements

The longitudinal and circumferential tensile strength tests of BC and SV-vascular grafts were performed according to the ISO-7198 standard using an MTS mechanical tester equipped with a 100 N load cell and operated at a speed of 50 mm/min. For the longitudinal tensile strength test, 5 cm BC and SV specimens were connected at both ends to Luer connectors (Nordson, US) using nonabsorbable braided 2.0 sutures (Ethicon, Germany) (Supplementary Fig. 2A). Before testing, the specimens were stretched to their rest position (zero load). The maximum longitudinal load (N) was recorded, and the longitudinal tensile stress (MPa) was calculated using Eq. (1) and reported.

$$\text{Longitudinal Tensile Stress (MPa)} = \frac{N}{\left[\pi \bullet \frac{\left(De^2 - Di^2\right)}{4}\right]} \quad (1)$$

where: N = force at breaking expressed in Newton (N). De = external diameter in mm. Di = internal diameter in mm.

For the circumferential tensile strength test, two rings (5 mm width) were cut at two extremities of each BC and SV vascular grafts were measured and placed between two parallel custom-made metal hooks (Supplementary Fig. 2B). Prior to testing, the specimens were stretched to a rest position (zero load). The maximum circumferential load (N) was reported, and the circumferential tensile stress (MPa) was calculated from Eq. (2) and reported.

$$\text{Circumferential Tensile Stress (MPa)} = \frac{N}{2 \bullet (L \bullet WT)} \quad (2)$$

where: N = force at breaking expressed in Newton (N). L = length of the sample in mm. WT = wall thickness in mm.

2.5. Suture retention measurements

Suture retention test was performed following the ISO-7198 standard using an MTS mechanical tester equipped with a 100 N load cell and operated at a speed of 50 mm/min. BC specimens, 5 cm long, were connected at one end to a Luer connector (Nordson, US). The opposite edge was sutured using a non-absorbable monofilament 6-0 suture thread (Ethibond, Ireland) inserted 2 mm from the upper cut edge. The free end of the suture was clamped to the MTS mechanical tester's crosshead (Supplementary Fig. 2C). Prior to testing, the specimens were stretched to a rest position (zero load). The maximum suture retention load (N) was recorded, and the suture retention stress (MPa) was calculated using Eq. (3) and reported.

$$\text{Suture Retention Stress (MPa)} = \frac{N}{(WT - T)\cdot \pi r} \quad (3)$$

where: N = force at breaking expressed in Newton (N). WT = wall thickness in mm. T = suture thickness wire in mm. r = suture radius in mm.

2.6. Burst pressure measurements

The burst pressure strength of SV and BC vascular grafts was recorded during increasing the pressure inside the specimen at a steady rate of 10 kPa/s until the graft burst occurred. BC (5 cm long) and SV (4 to 9 cm long) vascular graft samples were secured at both ends to Luer connectors (Nordson, US) with a nonabsorbable braided 2.0 suture (Ethicon, Germany). The inflation pressure was recorded using a pressure sensor (range: 199.9 – 1999 mbar; accuracy: ± 0.2 mbar) (Greisinger, Germany) (Supplementary Fig. 2D).

2.7. Dynamic radial compliance

Dynamic radial compliance tests of BC grafts were performed according to standard ISO-7198 using an advanced culture system already developed and employed at this scope (Supplementary Fig. 3A) [35,49]. The system can house a tubular sample inside an optical accessible culture chamber; the sample is secured to barbed connectors within the culture by means of silicon vessel loops and can be pre-tensioned using an adjustable shaft.

The fluid temperature (luminal and extraluminal) was maintained at 37 °C thanks to a heat exchanger consisting of a copper coil immersed in a thermostatic reservoir. Extraluminal fluid recirculation was achieved through a peristaltic pump (WP1000, Welco®, Japan) (Supplementary Fig. 3A).

Pulsatile pressure regime was achieved through a further peristaltic pump (luminal pump, WP1100, Welco®, Japan) and a proportional pinch-valve (S170XA01X2900VU, ASCO™, Italy) that compresses a silicone tube. The system received the pressure range set by the user and then it regulated the pinch-valve movement until the set pressure range, measured through a pressure sensor (PREPS-N-000, PendoTECH, US) was obtained.

During sample pulsatile pressurization, the system was positioned under a stereo microscope (Nikon SMZ1000) equipped with a high-speed camera (Miro Vision 2, Phantom, US) that was used for image acquisition. The collected images were analyzed using a Matlab sketch: the diameter dimension of each frame was calculated averaging the diameter in multiple points along the sample (Supplementary Fig.

3B–D).

Radial compliance (C, % 10^{-2} $mmHg^{-1}$) of BC vascular grafts ($n = 4$) was measured according to Eq. (4):

$$Compliance = \frac{\left(D_{P_{max}} - D_{P_{min}}\right)/D_{P_{min}}}{P_{max} - P_{min}} \cdot 10^4 \quad (4)$$

where: P_{max} and P_{min} = extremes of the pressure range of interest in mmHg. D_{Pmax} and D_{Pmin} = related internal diameters in mm.

BC vascular grafts' compliance was measured in the following ranges: 50–90, 80–120, and 110–150 mmHg, which mimic hypo-, normo-, and hypertension conditions, according to standard ISO 7198.

2.8. Histology and immunofluorescence staining

Bacterial DNA remaining content, cell infiltration, and BC scaffold remodeling were evaluated by Hematoxylin and Eosin (H&E) and immunofluorescent staining on sample slices. The specimens were washed with phosphate-buffered saline (PBS, Sigma-Aldrich, USA), fixed by overnight treatment with 4% paraformaldehyde (PFA, Sigma-Aldrich, USA), and sections of 10 μm in thickness were cut with a cryostat (Leica Biosystem CM1950, Leica Biosystem, Germany).

For the H&E staining, sample sections were stained using the Gemini autostainer (Thermo Fisher, USA) according to standard protocols. Images were acquired with a Nikon Ti2 inverted microscope (Nikon, Japan).

Immunofluorescence analysis was executed on sample slices following a standard protocol.

In detail, samples were washed with PBS (Sigma-Aldrich, USA), and they were incubated for 1 h at room temperature in 5% normal goat serum (Sigma-Aldrich, USA) with 0.25% Triton 100X (Sigma-Aldrich, USA) in PBS (Sigma-Aldrich, USA). After washing with PBS, samples were incubated for 1 h with the following primary antibodies: rabbit polyclonal IgG anti-CD45 (ab10558, Abcam, UK), mouse monoclonal IgG1 anti-CD68 (ab955, Abcam, UK) and mouse monoclonal IgG2a anti-vascular endothelial-cadherin (VE-cadherin, sc-52751, Santa Cruz Biotechnology, USA). Samples were again gently washed with PBS and consequently incubated in the dark for 30 min with fluorescently labeled Alexa 488 anti-rabbit, Alexa 647, and Alexa 546 anti-mouse secondary antibodies (Life Technologies, Thermo Fisher Scientific, USA). Nuclei were counter stained using 4′-6-diamino-2-phenylindole (DAPI, Sigma-Aldrich, USA) at 1:40 for 30 min. Incubations were performed at room temperature, and antibodies were diluted in PBS 1X with 0.1% bovine serum albumin (BSA, Sigma-Aldrich, USA). Primary and secondary antibodies dilution was 1:200. Images were acquired with a Nikon Ti2 inverted microscope (Nikon, Japan).

2.9. DNA quantification and fragment length analysis

To assess total DNA content within BC vascular grafts, 5 cm long specimens were blot dried, weighted, cut into thin strips, and digested with Proteinase K (Sigma-Aldrich, USA) at 56 °C overnight. Digested samples were centrifuged at 12000 rpm for 5 min to precipitate any remaining proteins. DNA content was quantified using CyQuant assay (Life Technologies, US) following the manufacturer's instructions. To determine DNA fragment size, samples were analyzed *via* microfluidics-based automated electrophoresis system (Agilent, US).

2.10. In vitro cytotoxicity assay

In vitro cytotoxicity assay was performed following ISO-10993. Human fibroblasts (Acharya et al., 2012) were plated and grown to 80% confluency prior to initiating the assay. For this test 0.1% ZDEC Polyurethan Film (FDSC, Japan) was used as a positive (cytotoxic) control. Cells cultured under normal conditions (without any material) were used as a blank control (blank). The materials (BC vascular graft and ZDEC) were incubated with the appropriate culture media at a concentration of 6 cm^2/mL for 48 h at 37 °C on a shaker. After 48 h, cell culture media was removed and replaced with the extract media. Cells were then incubated at 37 °C and 5% CO_2 for 24 h prior to cytotoxic evaluation with MTT cell metabolic activity assay (Sigma-Aldrich, USA).

2.11. Rotational thromboelastrometry (ROTEM) analysis

Rotational thromboelastometry (ROTEM) was performed to evaluate the effects of the BC vascular graft on whole blood coagulation. Fresh whole blood was collected from 1 healthy donor and anticoagulated with sodium citrate according to standard procedures.

BC vascular grafts ($n = 2$) were incubated in 0.9% NaCl (Fresenius Kabi, Japan) at a concentration of 6 cm^2/mL for 48 h at 37 °C under constant agitation to obtain material extracts. Control samples consisted of blood not exposed to the material extract. Blood sample was incubated with the BC vascular graft extract for 6 min prior to analysis. Following incubation, ROTEM analysis was carried out using a ROTEM® analyzer (Werfen, Spain) according to the manufacturer's instructions. Coagulation was initiated using a standard activation assay (Werfen, Spain), including INTEM and EXTEM to assess the intrinsic and extrinsic coagulation pathways, respectively. The parameters clotting time (CT), clot formation time (CFT), and maximum clot firmness (MCF) were recorded. ROTEM measurements were performed at 37 °C.

2.12. In vivo biological validation

All experiments were performed according to the Guide for the Care and Use of Laboratory Animals (National Institutes of Health Publication No. 85-23, revised 1996).

The experimental protocol was validated by the scientific committee for experimental research at the University of Verona and approved by the National Ministry of Health (Ministerial Authorization Number 82/2024-PR, Protocol Number 56DC9.94).

A total of 3 male Sprague Dawley rats weighing 400 ± 50 g, aged 5–6 months, were used. The rats were housed two in each cage with free access to food pellets and drinking water.

For the subcutaneous implants, 1 cm^2 of BC graft or Gore-Tex pieces were used.

Anesthesia was induced by Sevofluorane 6% (Forene, Abbot, Baar, Switzerland) mask anesthesia; animals were kept sedated using Oxygen and Sevofluorane 3%; Ketoprofen 2 mg/Kg (Artrosilene, Dompè Framaceutici, Italy) was subcutaneously injected to maintain analgesia. The skin on the back of the rats was shaved and disinfected with chlorexidine 2% (Chlorexinal 2%, Candioli Pharma, Italy). A 5 cm long incision was made on the back of the animals. Four subcutaneous pockets were carefully prepared with forceps. Implants were inserted into the pockets with fixation, using a 6-0 Prolene (Ethicon Inc., Johnson&Johnson, USA). The skin was sutured with 2-0 Ti-Cron (Ethicon Inc., Johnson&Johnson, USA).

BC and Gore-Tex implants were explanted 4 weeks after implantation. The animals were given Sevofluorane 6% (Forene, Abbot, Baar, Switzerland) by inhalation before the explant procedure. All implants were explanted with the surrounding tissue.

2.13. Statistical analyses

Data are expressed as a mean ± standard error of the mean (SEM) of at least three different experiments. Statistical comparisons were performed with either paired or unpaired Student's *t*-test; p; *, $p < 0.05$; **, $p < 0.01$; ***, $p < 0.001$; ****, $p < 0.0001$; ns, not significant.

The confidence interval (CI) for the median of key mechanical (burst pressure strength $n = 6$, circumferential $n = 8$ and tensile $n = 7$ strength) and morphological (wall thickness $n = 24$ and outer diameter n = 24) properties of different BC graft batches was computed with a nominal confidence level of 95% to underscore the reproducibility of the

production process. GraphPad Prism 10 (v 10.5.0) was used for the statistical analyses.

3. Results

3.1. Saphenous vein (SV) morphology and mechanical properties

SV was analyzed in terms of morphology and mechanical properties to serve as a benchmark for comparison with engineered BC-grafts. Spare segments of SV were collected from patients undergoing CABG procedures and characterized accordingly. The average length of the collected SV segments was 5.4 ± 4.7 cm. A majority (61.5%) of the samples exhibited multiple side branches, which were sealed with metallic clips, averaging 3.1 ± 2.3 clips per graft (Fig. 1A).

Morphological measurements revealed an inner diameter (ID) of 2.6 ± 0.7 mm, an outer diameter (OD) of 4.9 ± 1.3 mm, and a wall thickness (WT) of 0.55 ± 0.084 mm (Fig. 1B). Notably, both inter-donor and intra-graft variability were observed in these parameters, highlighting the inherent heterogeneity of autologous veins.

In terms of mechanical performance, SV grafts exhibited a burst pressure strength of 577.4 ± 631.3 mmHg (Fig. 1C), with significant variations among donors. Circumferential tensile strength was 1.856 ± 1.021 MPa, while longitudinal tensile strength reached 26.07 ± 7.23 MPa (Fig. 1D).

Overall, SV grafts demonstrated considerable variability in both morphological and mechanical properties. This heterogeneity can critically affect graft durability, mechanical matching with native vessels, and the long-term patency and performance of the grafts when used as conduits in CABG.

3.2. Bacterial cellulose vascular graft morphology and mechanical properties

Morphology and mechanical properties, such as burst pressure, tensile strength, suturability, and compliance, are critical parameters for evaluating the performance of artificial vascular grafts.

Engineered BC vascular grafts were successfully generated as uniform, branch-free tubular structures without clips (Fig. 2A). Each graft measured 15 cm in length with a consistent nominal ID of 4 mm, a WT of 0.46 ± 0.05 mm, and an OD of 4.92 ± 0.10 mm (Fig. 2F).

The BC graft wall consisted of multiple layers oriented parallel to the luminal and external surfaces. SEM imaging at different magnifications revealed these distinct layers (Fig. 2B–C) as well as the characteristic nanofiber architecture of BC scaffolds (Fig. 2D–E). The inner luminal surface exhibited a network of thin, interwoven fibers (Fig. 2D), while the outer surface showed thicker, flattened fibers, that formed a smoother layer (Fig. 2E).

The burst pressure strength of BC grafts was 306.6 ± 96.0 mmHg (Fig. 2G), which was lower than that of the human SV grafts (688.60 ± 690.34 mmHg, Fig. 1C).

BC grafts exhibited circumferential tensile strength of 0.39 ± 0.18 MPa (Fig. 2H) and longitudinal tensile strength of 0.24 ± 0.15 MPa (Fig. 2H). The elongation at failure was 5.4 ± 1.6% in the circumferential direction and 0.78 ± 0.98% longitudinally (Fig. 2I).

The suture retention strength was 0.04 ± 0.02 MPa (Fig. 2H), and the elastic modulus in the circumferential direction was 2.64 ± 1.73 MPa (Supplementary Fig. 4).

Radial compliance, a critical factor for small diameter (<6 mm) vascular grafts, reflects the graft's ability to change in response to intraluminal pressure variations. BC grafts showed radial compliance values of 0.90 ± 0.11% /100 mmHg under hypotensive blood pressure (50–90 mmHg), 0.75 ± 0.28% /100 mmHg under normotensive pressure (80–120 mmHg), and 0.72 ± 0.25% /100 mmHg under hypertensive pressure (110–150 mmHg) (Fig. 2J).

The CIs for the median of key mechanical and morphological properties, computed with a nominal confidence level of 95%, showed actual confidence levels greater than 95%, indicating conservative estimations and low variability in the observed values. Specifically, the actual confidence levels were 96,88% (lower confidence limit (LCL) = 118.5, upper confidence level (UCL) = 421.5) for burst pressure strength;

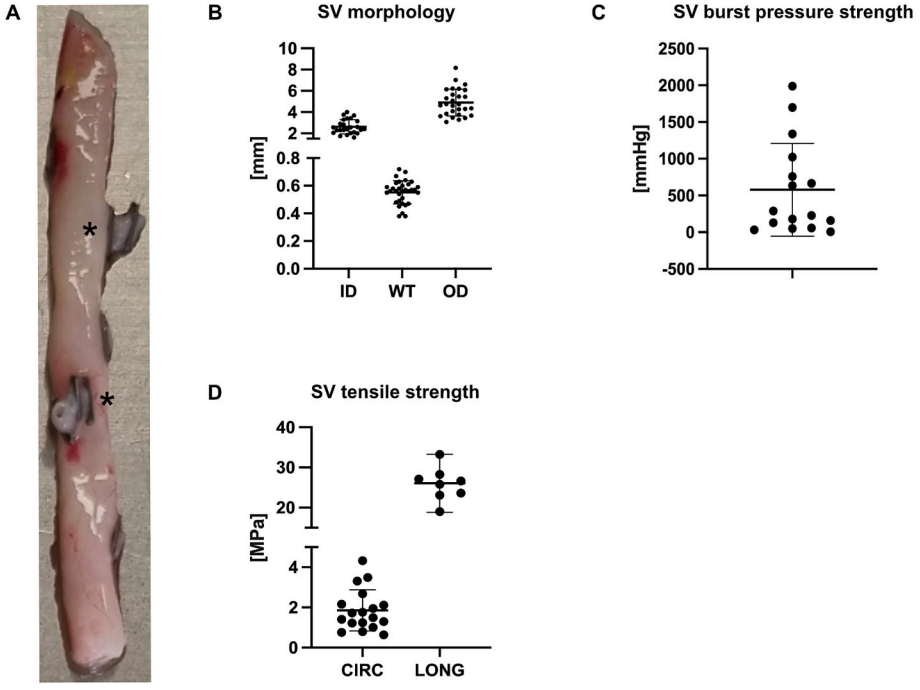

Fig. 1. SV graft morphological and mechanical properties: **A)** Macroscopic picture of collected SV graft. * indicates side branches closed with metallic clips; **B)** SV morphological features: inner diameter (ID) ($n = 25$), wall thickness (WT) ($n = 33$) and outer diameter (OD) ($n = 28$); **C)** SV graft burst pressure strength considered as the amount of internal pressure a graft can withstand before the graft bursts ($n = 16$); **D)** SV tensile strength properties, in particular circumferential (CIRC) ($n = 18$) and longitudinal (LONG) ($n = 10$).

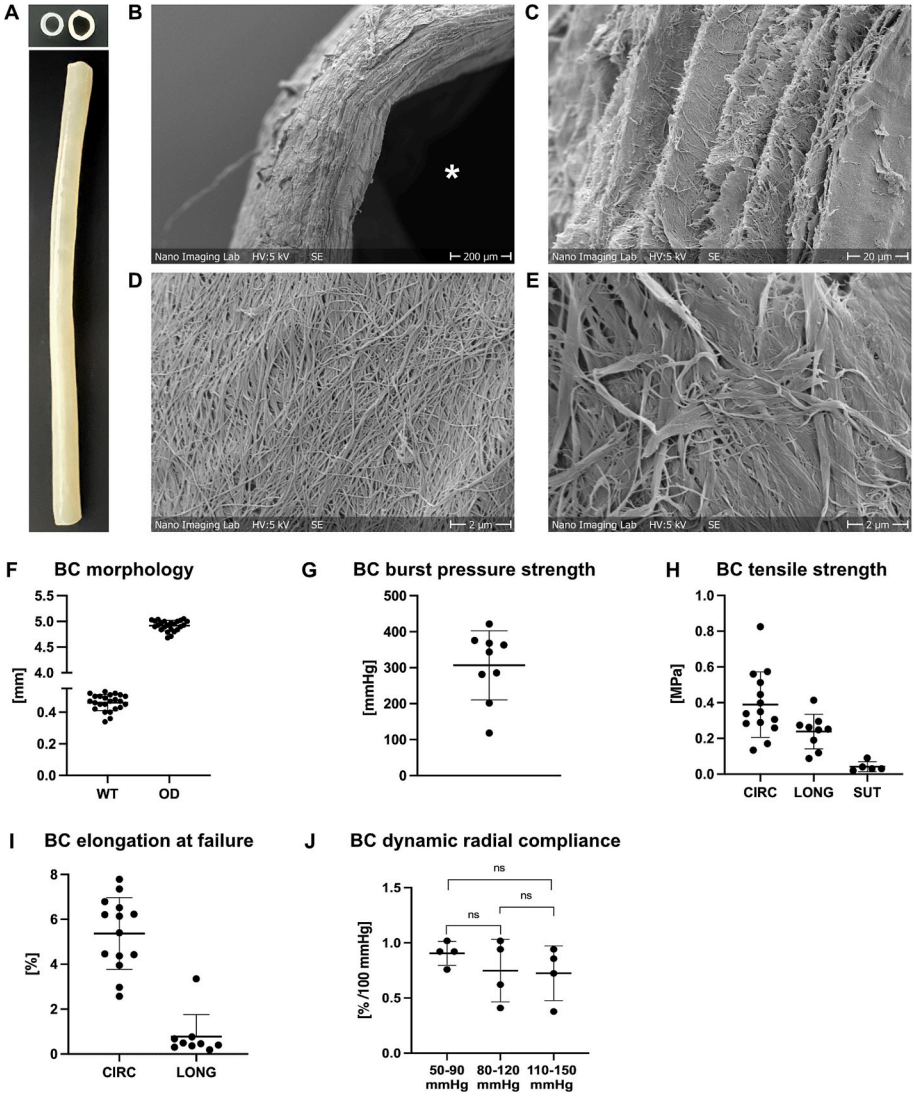

Fig. 2. BC graft morphological and mechanical properties: **A)** BC graft cross section (top right) compared with a silicone tube (top left, 3 mm inner ∅ and 0.5 mm wall thickness) and BC graft 10 cm long piece; **B)** BC graft cross section Scanning Electron Microscopy (SEM). * indicates the BC graft lumen; **C)** The enlargement shows the multilayered structure of the BC graft wall; **D)** SEM of BC luminal inner side; **E)** SEM image of BC graft outer surface; **F)** BC morphological features: wall thickness (WT) and outer diameter (OD) ($n = 24$); **G)** BC graft burst pressure strength considered as the maximum internal pressure a graft can withstand before failure ($n = 9$); **H)** BC tensile strength properties: circumferential (CIRC) ($n = 14$), longitudinal (LONG) (n = 9) tensile strength, and suture retention strength (SUT) ($n = 5$); **I)** Circumferential (CIRC) (n = 14) and longitudinal (LONG) (n = 9) BC elongation at failure; **J)** BC graft dynamic radial compliance at hypotensive, normotensive, and hypertensive blood pressure levels ($n = 4$). Shapiro-Wilk Test was performed for statistical analysis ($p = 0.05$).

99.2% (LCL = 0.153, UCL = 0.825) for circular tensile strength; 98.44% (LCL = 0.088, UCL = 0.338) for longitudinal tensile strength; 97.73% (LCL = 0.43, UCL = 0.50) for wall thickness; and 97.73% (LCL = 4.85 and UCL = 5.00) for outer diameter.

Overall, BC vascular grafts showed greater uniformity and reproducibility in both morphology and mechanical performance compared to SV grafts, supporting their potential as standardized small caliber vascular substitutes.

3.3. *In vitro assessments of BC vascular grafts: residual biological material, cytotoxicity and thrombogenicity*

To evaluate cytocompatibility, BC grafts were analyzed for residual bacterial DNA content, which is directly associated to adverse host reactions, as well as cytotoxicity. Histological analysis using H&E (Fig. 3A–B) and DAPI (Fig. 3C–D) staining revealed no detectable nuclear material following NaOH treatment, indicating effective removal of residual cellular content.

To minimize adverse cellular and host responses, decellularized biological scaffolds composed of ECM should contain less than 50 ng of double-stranded DNA (dsDNA) per milligram of tissue dry weight, with DNA fragments shorter than 200 base pair (bp) [36].

BC grafts met these criteria, with an average residual DNA content of 16.66 ± 13.58 ng per milligram of BC dry weight (Fig. 3E), and detected DNA fragments length under 200 bp (Fig. 3F).

Cytotoxicity was assessed using *in vitro* viability assay (Fig. 3G), which demonstrated no significant cytotoxic effects, with a mean cell viability of 73.79 ± 10.95%. While ISO 10993-5 does not define strict pass/fail thresholds for cytotoxicity testing, a cell survival rate above 70% or higher is widely accepted as indicative of non-cytotoxicity (ISO 10993-5) [37].

Rotational thromboelastometry (ROTEM) was used to assess the viscoelastic properties of whole blood after contact with BC-vascular graft.

No significant differences were observed in clotting time (CT), clot formation time (CFT), or maximum clot firmness (MCF) between blood

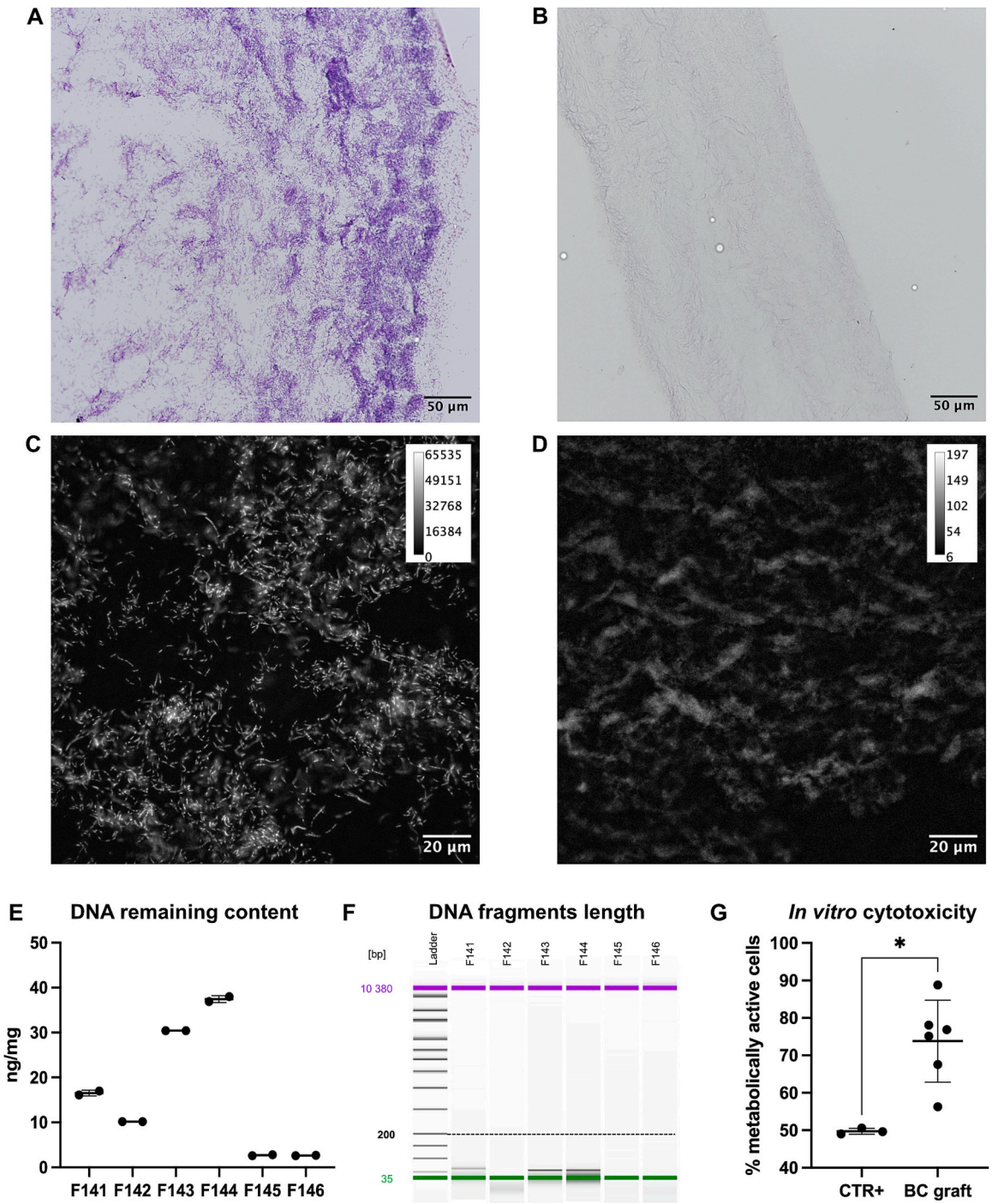

Fig. 3. BC graft *in vitro* assessments of biological material residual and cytotoxicity: **A)** H&E staining before bacteria removal (n = 4); **B)** H&E staining after bacteria removal (n = 4). Scale bar = 50 μm. **C)** BC graft section stained with DAPI before bacteria removal (n = 4); **D)** BC graft section stained with DAPI after bacteria removal (n = 4). Scale bar = 20 μm. Note the intensity scale bar, the signal represents BC graft autofluorescence; **E)** CyQuant assay performed to quantify the bacteria DNA remaining content after bacteria removal (n = 6); **F)** Bacteria DNA fragments length assessment after bacteria removal (n = 6); **G)** BC graft cytotoxicity evaluation with MTT cell metabolic activity assay (n = 6). 0.1% ZDEC polyurethane film served as positive (cytotoxic) control (CTR+).

exposed to BC-vascular graft and control samples (Supplementary Table 1).

In summary, the BC grafts demonstrated low residual DNA content, no visible nuclear material, and acceptable cytocompatibility, and no detectable alterations in blood coagulation *in vitro*, supporting their suitability for further *in vivo* evaluation and potential use as implantable medical devices.

3.4. *In vivo* biocompatibility of bacterial cellulose (BC) vascular grafts

BC vascular graft explants were assessed for inflammation, foreign body responses, and cell infiltration.

After 4 weeks of subcutaneous implantation, no macroscopic signs of inflammation, such as redness, edema, or exudate, were observed around the BC explants (Supplementary Fig. 5A).

Histological analysis with H&E staining revealed a subacute inflammatory response, characterized by granulation tissue formation, a

typical reparative process following implantation of foreign materials (Fig. 4A). This organized tissue included newly formed blood vessels, fibroblasts, and a heterogeneous population of inflammatory cells, primarily lymphocytes, along with some histiocytes, occasional neutrophils, and eosinophils.

For comparison, Gore-Tex®, a clinically used synthetic material in applications with blood-contact, was implanted under similar conditions (Supplementary Fig. 5B). After 4 weeks, Gore-Tex® explants exhibited granulation tissue primarily composed of fibroblasts and lymphocytes, indicative of a moderate chronic inflammatory response (Fig. 4B). In both BC and Gore-Tex® groups, necrotic cellular debris, likely originating from neutrophils, was observed in tissue immediately surrounding the implants.

The potential for calcification was also assessed at the 4-week time point. No hydroxyapatite deposits were detected in the BC explants (Fig. 4C,) whereas calcific deposits were observed in the Gore-Tex® group (Fig. 4D), suggesting a lower tendency for mineralization in BC vascular grafts.

4. Discussion

The development of small-diameter artificial blood vessels remains a major challenge in vascular tissue engineering, highlighting the urgent need for alternatives to overcome limitations in production, characterization, and clinical translation. This study aimed to develop a BC-based small-diameter vascular graft as a consistent, reproducible, and scalable solution, capable to address these critical steps.

Previous efforts have focused on optimizing BC vascular graft fabrication. For example, Weber *et al.* (2017) increased graft length to approximately 10 cm and reduced wall thickness to 1–2.5 mm compared with first-generation BC grafts, which exhibited wall thicknesses of 2–3.5 mm [22]. While these advances represented important progress, limitations in production time, structural uniformity, and scalability remained [24].

Our approach is technically innovative compared to conventional methods used in other studies [8,22–24,28–30], which often rely on oxygen gradient-dependent deposition in rotating or air-liquid interface cultures [24,28]. In our study, we implemented a closed single culture chamber with a silicone tubing system to deliver oxygen, but differently from the other approaches, we used a horizontal rotating system with high-concentration oxygen to facilitate even cellulose wrapping around the tubing instead of vertical static systems [28]. Although the results were comparable in terms of wall thickness, biocompatibility, and mechanical properties, grafts obtained under static conditions required a significantly longer culture period (over 14 days *vs.* 5 days in our study) [23,24,28]. Additionally, cellulose layers in static cultures exhibited

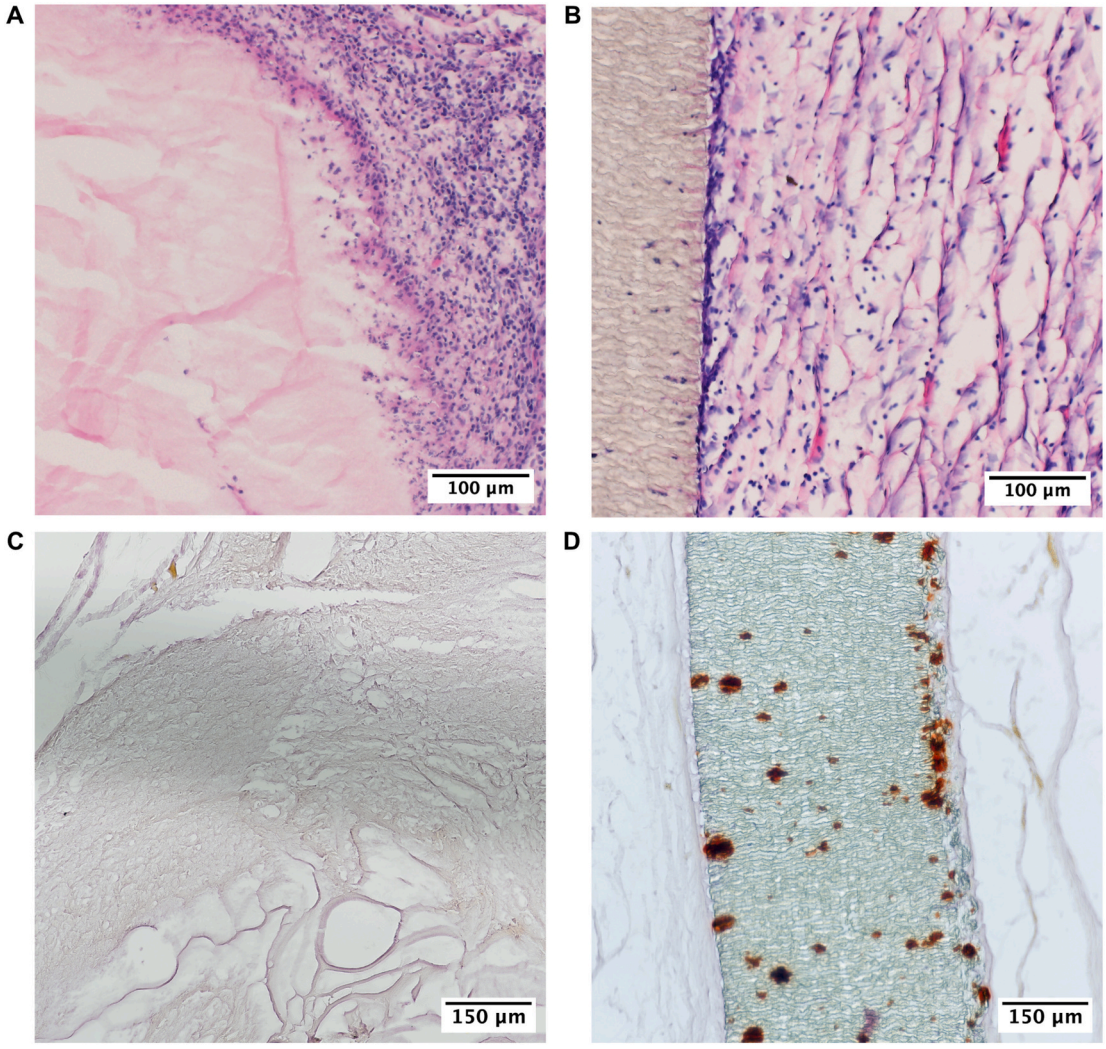

Fig. 4. BC graft *in vivo* biocompatibility: Representative images for H&E staining of **A)** BC graft explants and **B)** Gore-Tex explants implanted subcutaneously for 4 weeks (n = 4). Scale bar = 100 µm. Representative images for Alizarin Red staining of **C)** BC graft explants and **B)** Gore-Tex explants implanted subcutaneously for 4 weeks (n = 4). Scale bar = 150 µm. (For interpretation of the references to colour in this figure legend, the reader is referred to the web version of this article.)

inconsistencies, with some areas having loosely packed fibers and others being denser, increasing the risk of delamination and aneurysm formation. In contrast, our constructs featured a denser and more uniform structure, enhancing their mechanical integrity. Furthermore, our approach enabled the production of longer grafts compared to previous studies. While earlier studies were limited to graft lengths of approximately 14 cm, constrained by the length of 14 cm of the silicone tube [28], our approach produced grafts with a useable length of up to 15 cm after harvesting, edge trimming, and decellularization. The resulting BC grafts exhibited uniform inner diameter and wall thickness, parameters that are critical for clinical translation. Importantly, the system is readily adaptable to different inner diameters (<6 mm) and extended lengths (up to 20 cm), highlighting its scalability and versatility.

Although a similar concept has been used in engineering short cartilage tubular blocks *via* vertically positioned oxygen sources [28,31], our system focuses on the efficient production of long, small-diameter tubular grafts with high reproducibility in terms of mechanical properties and morphological features. Additionally, the establishment of a bacterial cell bank, along with the implementation of quality control criteria to assess bacterial and cellulose deposition before starting the fermentation process helped in improving the control of the fermentation process and increase reproducibility. Although these tests for these specific parameters are known [32], these are not often implemented during the production process as quality criteria of the production. Together with the regulation and control over some key parameters that often are not disclosed or not controlled at all such as the concentration of BC used for fermentation process, further advances the state of the art and enhance the standardization and scalability of the production process.

Compared to other tissue-engineered vascular grafts, notably Humacyte®, BC grafts offer key advantages in terms of production speed, scalability, and cost-efficiency. Humacyte grafts are developed by seeding human vascular cells onto biodegradable scaffolds, followed by weeks to months of cell culture and decellularization to preserve ECM while removing immunogenic material [13–15,38]. This process is time- and resource-intensive due to the reliance on human cell availability and expansion.

In contrast, BC grafts are produced in just 5 days using bacteria, which are easy to culture, expand, and store, enabling rapid, large-scale manufacturing. This makes BC grafts particularly attractive for off-the-shelf applications and more accessible in low-resource settings.

Currently, autologous blood vessels, such as the mammary artery, SV, radial artery, and cephalic vein, remain the only available options for small-diameter blood vessel replacement. While arteries are considered the gold standard, SV is often used in over 90% of CABG procedures due to its length, and accessibility, especially in the case of multiple by-passes [39] [40].

However, their inherent biological variability, including the presence of valves and differences in wall structure, might lead to inconsistent mechanical performance. This study directly compared BC grafts with SV as a benchmark for the first time, confirming these limitations by subjecting SV remnants from CABG surgeries to rigorous mechanical testing, highlighting significant intra- and inter- sample variability despite identical testing protocols. Although SV mechanical properties were consistent with previously reported data [33,41], such variability underscores the need for engineered vascular grafts with predictable and reproducible properties.

While their mechanical properties currently fall short of autologous blood vessels, the grafts exhibited high reproducibility across samples, addressing a critical challenge in vascular graft production. Importantly, the characterization of cell-free BC grafts occurs prior to *in vivo* implantation, suggesting that their mechanical properties could further improve post implantation as they undergo remodeling by autologous cells and newly deposited ECM. This remodeling process has the potential to enhance graft durability and integration within the host vasculature [22–24,29]. For artificial blood vessels to be clinically relevant, they must withstand both physiological and pathological pressure ranges, resisting to pulsatile flow without rupturing. Burst pressure, which measures the maximum pressure a scaffold can withstand before failure, is a key parameter for assessing graft suitability [42]. BC-based graft burst pressure (306.6 ± 96.04 mmHg) is within ranges of other BC vascular grafts [28] and exceeded physiological and pathological pressure thresholds, highlighting their potential for safe clinical application.

One of the key challenges in artificial vascular grafts is achieving a dynamic radial compliance that closely matches natural vessels, as mismatched compliance can compromise graft function and long-term patency [43]. The BC vascular graft radial compliance (0.792 ± 0.09%/100 mmHg), although lower than that of natural tissues such as human SV (4.40 ± 0.80%/100 mmHg; [44]), and carotid artery (14%/100 mmHg; [45]), was comparable to commercially available synthetic materials used in large-diameter vascular grafts, such as ePTFE (0.90 ± 0.10; [46]) and Dacron (1.90 ± 1.20; [46]). These findings suggest that BC grafts represent a promising starting point for further optimization in terms of mechanical performances.

In vitro and *in vivo* findings reinforced the biocompatibility of this bio-based BC material [47]. *In vitro* testing confirmed that the protocol for removing bacterial residues from the fibrillar network of cellulose effectively preserves its biocompatibility. However, variability in DNA residue content and cytotoxicity observed across samples highlights the need for Good Manufacturing Practice (GMP)-compliant production facilities to support consistent quality for clinical use. Subcutaneous implantation of BC grafts revealed only mild inflammatory response and no calcification, in contrast to Gore-Tex control, which showed both chronic inflammatory features and mineral deposition.

Thrombogenicity represents a key translational challenge for small-diameter vascular grafts. In the present study, the *in vitro* thrombogenicity testing yielded results consistent with previous reports demonstrating excellent hemocompatibility of BC-based grafts [25,37]. However, *in vivo* thrombogenic assessment remains critical. Notably, Fusco *et al.* reported that BC grafts implanted *in vivo* in a porcine model were capable of integrating with native tissue, exhibiting significant colonization by autologous cells without any signs of thrombosis or luminal narrowing [23]. In a 4-week CABG model in pigs, BC grafts with a 4-mm-inner diameter and an embedded Cobalt-Chrome (CoCr) mesh remained patent, indicating their ability to withstand physiological conditions while supporting cellular infiltration and ECM deposition. In the current production process, the embedding of the CoCr mesh was not included and is instead considered as an optional external support, to be applied based on the surgeon's discretion at the time of implantation. Future investigations may explore additional approaches to reinforce BC and more closely match the mechanical properties of native arteries, such as the incorporation of fibroin [48]. Long-term *in vivo* studies in large animal models are still required to fully assess durability, thrombogenicity and patency. Nevertheless, these findings support the notion that cell-free BC grafts function as biologically responsive platforms, capable of *in vivo* remodeling and integration. This is a critical attribute for long-term graft success, as the infiltration of host cells and progressive extracellular remodeling may further enhance the mechanical strength and functional performance of the implanted grafts over time.

5. Conclusion

This study presents a robust and scalable method for producing small-diameter BC vascular grafts with high morphological uniformity, favorable mechanical properties, and excellent biocompatibility. These engineered grafts offer a promising translational alternative owing clinically relevant size.

Beyond CABG, BC-based vascular grafts hold potential for use in other vascular procedures, including non coronary bypass surgery or endovascular applications or arteriovenous shunts, pending further adaptation and testing. Further *in vivo* validation in arterial

environments and long-term studies are essential to confirm remodeling capacity, mechanical stability, and long-term patency. Ultimately, BC grafts represent a versatile and clinically relevant option for revascularization strategies across a range of indications, with potential applicability in both adult and pediatric patients.

CRediT authorship contribution statement

Deborah Fusco: Writing – review & editing, Writing – original draft, Visualization, Validation, Methodology, Formal analysis, Data curation, Conceptualization. **Noor Christiaens:** Methodology, Formal analysis. **Elia Pederzani:** Writing – review & editing, Methodology, Formal analysis, Data curation. **Sara Martinazzi:** Writing – review & editing, Methodology, Formal analysis. **Giuseppe Isu:** Writing – review & editing, Supervision, Methodology, Conceptualization. **Florian Meissner:** Writing – review & editing, Methodology, Conceptualization. **Jules Miazza:** Writing – review & editing, Methodology. **Urs Zenklusen:** Writing – review & editing, Methodology. **Michael Gregor:** Writing – review & editing, Methodology, Formal analysis. **Luca Koechlin:** Writing – review & editing, Methodology. **Alessia Pisanu:** Writing – review & editing, Methodology, Formal analysis. **Marcello Raimondi Lucchetti:** Writing – review & editing, Methodology. **Gianfranco B. Fiore:** Writing – review & editing, Methodology, Formal analysis. **Monica Soncini:** Writing – review & editing, Methodology, Formal analysis. **Katharina Glatz:** Writing – review & editing, Formal analysis, Data curation. **Alessio Rungatscher:** Writing – review & editing, Methodology, Formal analysis. **Bernhard Winkler:** Writing – review & editing, Methodology, Conceptualization. **Friedrich Eckstein:** Writing – review & editing, Writing – original draft, Supervision, Methodology, Funding acquisition, Conceptualization. **Anna Marsano:** Writing – review & editing, Writing – original draft, Validation, Supervision, Project administration, Methodology, Data curation, Conceptualization.

Declaration of competing interest

The authors declare that they have no known competing financial interests or personal relationships that could have appeared to influence the work reported in this paper.

Acknowledgements

This work was financially supported by the Department of Cardiac Surgery at the University Hospital of Basel. The authors would like to thank Philip Dettinger (Department of Biomedicine, Basel, Switzerland) for his technical and scientific support regarding the bioreactor; Stefano Gabetti (Politecnico di Torino, Turin, Italy), Beatrice Antigone Rossi (Politecnico di Milano, Milan, Italy), Silvia Riboldi (Politecnico di Milano, Milan, Italy), Alessia Sofia Bolandrina (Politecnico di Milano, Milan, Italy), Lucrezia Moro (Politecnico di Milano, Milan, Italy) and Beat Göpfert (Department of Biomedical Engineering, Basel, Switzerland) for the valuable scientific and technical support in the mechanical tests; Roy Allenspach (Department of Biomedicine, Basel, Switzerland) for his support at the organizational level; Brigitta Gahl (University Hospital of Basel, Basel, Switzerland) for her statistical expertise; Gregory Reid (Department of Biomedicine, Basel, Switzerland) for assisting with the ethical application for the study on human saphenous veins; Daniel Gauss for his contribution during a curricular internship; Christian Fusco (Politecnico of Torino, Turin, Italy) for his valuable help in preparing the Supplementary Fig. 1; Ewelina Bartoszek-Kandler (Microscopy facility – Department of Biomedicine, Basel, Switzerland) for her essential assistance with microscopy; Mylène Toranelli and Diego Calabrese (Histology Core Facility – Department of Biomedicine, Basel, Switzerland) for their technical contribution in histology; Eva Bieler (Department of Physics (SNI), Basel, Switzerland) for her technical expertise regarding scanning electron microscopy; Giulia Milan (Department of Biomedicine, Basel, Switzerland), Barbara Kappeller (Institute of Biomedical Research of Vienna, Vienna, Austria) and Bruno Podesser (Institute of Biomedical Research of Vienna, Vienna, Austria) and Martin Grapow (Department of Surgery, University Hospital of Basel) for the scientific and clinical discussion, and Daniele Linardi (Department of Surgery – University of Verona, Verona, Italy) for their support in the animal model. Servier Medical Art was used to create the graphical abstract, which is licensed under CC BY 4.0 (https://creativecommons.org/licenses/by/4.0/).

Appendix A. Supplementary data

Supplementary data to this article can be found online at https://doi.org/10.1016/j.bioadv.2026.214851.

Data availability

Data will be made available on request.

References

[1] S.S. Martin, et al., 2024 heart disease and stroke statistics: a report of US and global data from the American Heart Association, Circulation 149 (8) (2024) e347–e913.
[2] A. Timmis, et al., European society of cardiology: cardiovascular disease statistics 2019, Eur. Heart J. 41 (1) (2020) 12–85.
[3] D.G. Seifu, et al., Small-Diameter Vascular Tissue Engineering, 2013.
[4] A. Farber, Chronic limb-threatening ischemia, N. Engl. J. Med. 379 (2018) 171–180.
[5] A.G. Alonso, et al., Alternative access for peripheral vascular interventions, J. Vasc. Surg. Cases Innov. Tech. 9 (2023) 101232.
[6] J.F. Sabik, Understanding saphenous vein graft patency, Circulation 124 (2011) 273–275.
[7] P. Mallis, et al., Future perspectives in small-diameter vascular graft engineering, Bioengineering 7 (2020) 1–40.
[8] J. Wippermann, et al., Preliminary Results of Small Arterial Substitute Performed with a New Cylindrical Biomaterial Composed of Bacterial Cellulose, 2009.
[9] R.H. Liu, et al., Review of vascular graft studies in large animal models, Tissue Eng. Part B Rev. 24 (2018) 133–143.
[10] J. Chen, et al., Current strategies for engineered vascular grafts and vascularized tissue engineering, Polymers 15 (9) (2023).
[11] Z.Y. Wang, S.M. Mithieux, A. Weiss, Fabrication techniques for vascular and vascularized tissue engineering, Adv. Healthc. Mater. 8 (19) (2019).
[12] S. Pashneh-Tala, S. MacNeil, F. Claeyssens, The tissue-engineered vascular graft-past, present, and future, Tissue Eng. Part B Rev. 22 (1) (2016) 68–100.
[13] Williams Adam R., et al., Acellular tissue engineered vessels as coronary artery bypass grafts, JACC: Basic Transl. Sci. 10 (2025).
[14] S. Cifuentes, et al., Outcomes of lower extremity arterial bypass using the human acellular vessel in patients with chronic limb-threatening ischemia, J. Vasc. Surg. 79 (2) (2024) 348–357 e2.
[15] J.J. Morrison, et al., Clinical implementation of the Humacyte human acellular vessel: implications for military and civilian trauma care, J. Trauma Acute Care Surg. 87 (1S Suppl 1) (2019) S44–S47.
[16] J. Wang, et al., Bacterial cellulose production, properties and applications with different culture methods – a review, Carbohydr. Polym. 219 (2019) 63–76.
[17] C. Zhong, Industrial-scale production and applications of bacterial, Cellulose 8 (2020) 1–19.
[18] M. Moniri, et al., Production and status of bacterial cellulose in biomedical engineering, Nanomaterials 7 (2017) 1–26.
[19] P. Gatenholm, D. Klemm, Bacterial nanocellulose as a renewable material for biomedical applications, MRS Bull. 35 (3) (2010) 208–213.
[20] A. Stanisławska, Bacterial nanocellulose as a microbiological derived nanomaterial, Adv. Mater. Sci. 16 (2016) 45–57.
[21] K. Dawidowska, et al., In vitro study of a stentless aortic bioprosthesis made of bacterial cellulose, Cardiovasc. Eng. Technol. 11 (2020) 646–654.
[22] C. Weber, et al., Patency and in vivo compatibility of bacterial nanocellulose grafts as small-diameter vascular substitute, J. Vasc. Surg. 68 (6S) (2018) 177S–187S.
[23] D. Fusco, et al., Small-diameter bacterial cellulose-based vascular grafts for coronary artery bypass grafting in a pig model, Front. Cardiovasc. Med. 9 (2022) 881557.
[24] M. Scherner, et al., application of tissue-engineered blood vessels of bacterial cellulose as small arterial substitutes: proof of concept? J. Surg. Res. 189 (2) (2014) 340–347.
[25] S. Zang, et al., Investigation on artificial blood vessels prepared from bacterial cellulose, Mater. Sci. Eng. C Mater. Biol. Appl. 46 (2015) 111–117.
[26] G. Helenius, et al., In vivo biocompatibility of bacterial cellulose, J. Biomed. Mater. Res. A 76 (2006) 431–438.
[27] J. Phan, Production Design and Evaluation of Vascular Grafts made of Bacterial Cellulose, Master of science thesis in the master degree program, biotechnology, 2010.

[28] L. Bao, et al., Physicochemical properties and in vitro biocompatibility of three bacterial nanocellulose conduits for blood vessel applications, Carbohydr. Polym. 239 (2020) 116246.
[29] Y. Li, et al., Construction of small-diameter vascular graft by shape-memory and self-rolling bacterial cellulose membrane, Adv. Healthc. Mater. 6 (11) (2017).
[30] Alexandre F. Leitão, et al., A novel small-caliber bacterial cellulose vascular prosthesis: production, characterization, and preliminary in vivo testing, Macromol. Biosci. 16 (1) (2016) 139–150.
[31] J.Y. Tang, et al., Comparison of two types of bioreactors for synthesis of bacterial nanocellulose tubes as potential medical prostheses including artificial blood vessels, J. Chem. Technol. Biotechnol. 92 (6) (2017) 1218–1228.
[32] V.T. Nguyen, et al., Spontaneous mutation results in lower cellulose production by a strain from Kombucha, Carbohydr. Polym. 80 (2) (2010) 337–343.
[33] P. Lestari, Study on the production of bacterial cellulose from acetobacter xylinum using agro-waste, Jordan J. Biol. Sci. 7 (2014) 75–80.
[34] B.A. Hamedani, et al., Comparison Between Mechanical Properties of Human Saphenous Vein and Umbilical Vein, 2012.
[35] E. Pederzani, et al., An Advanced Culture System to Investigate Electrospun Graft Biomechanisms for Vascular Tissue Engineering, 2023.
[36] P.M. Crapo, T.W. Gilbert, S.F. Badylak, An overview of tissue and whole organ decellularization processes, Biomaterials 32 (12) (2011) 3233–3243.
[37] H. Kanďárová, et al., The "Big Three" in biocompatibility testing of medical devices: implementation of alternatives to animal experimentation—are we there yet? Front. Toxicol. 5 (2023) 1–9.
[38] R.D. Kirkton, et al., Bioengineered human acellular vessels recellularize and evolve into living blood vessels after human implantation, Sci. Transl. Med. 11 (485) (2019).
[39] T.A. Schwann, et al., Operative outcomes of multiple-arterial versus single-arterial coronary bypass grafting, Ann. Thorac. Surg. 105 (2018) 1109–1119.
[40] N. Samano, et al., Saphenous veins in coronary artery bypass grafting need external support, Asian Cardiovasc. Thorac. Ann. 29 (2021) 457–467.
[41] G. Konig, et al., Mechanical properties of completely autologous human tissue engineered blood vessels compared to human saphenous vein and mammary artery, Biomaterials 30 (2009) 1542–1550.
[42] S.H. Kim, et al., Mechanical properties of compliant double layered poly(L-lactide-co-ε- caprolactone) vascular graft, Macromol. Res. 21 (2013) 886–891.
[43] O. Castillo-Cruz, et al., Prediction of circumferential compliance and burst strength of polymeric vascular grafts, J. Mech. Behav. Biomed. Mater. 79 (2018) 332–340.
[44] J.E. Puskas, Y. Chen, Biomedical application of commercial polymers and novel polyisobutylene-based thermoplastic elastomers for soft tissue replacement, Biomacromolecules 5 (4) (2004) 1141–1154.
[45] S.Q. Liu, M. Kodama, Porous polyurethane vascular prostheses with variable compliances, J. Biomed. Mater. Res. 26 (11) (1992) 1489–1502.
[46] N.R. Tai, et al., Compliance properties of conduits used in vascular reconstruction, Br. J. Surg. 87 (11) (2000) 1516–1524.
[47] S.M. Choi, et al., Bacterial cellulose and its applications, Polymers 14 (2022).
[48] K. Wang, et al., Preparation of bacterial cellulose/silk fibroin double-network hydrogel with high mechanical strength and biocompatibility for artificial cartilage, Cellulose 27 (2020) 1845–1852.
[49] E. Pederzani, et al., An Automated Modular Platform for Vascular Graft Assessment via Coronary-like Flow-Induced Stimulation, Bioengineering 113 (2) (2026) 221.